

Long-Term Radioiodine Retention and Regression of Liver Cancer after Sodium Iodide Symporter Gene Transfer in Wistar Rats

Jamila Faivre,¹ Jérôme Clerc,^{1,2} René Gérolami,³ Julie Hervé,¹ Michèle Longuet,¹ Bingkai Liu,¹ Jérôme Roux,⁴ Frédéric Moal,⁴ Michel Perricaudet,⁵ and Christian Bréchet¹

¹Department of Liver Cancer and Molecular Virology, Institut National de la Santé et de la Recherche Médicale Unit 370, Paris V University, CHU Necker, Paris; ²Department of Nuclear Medicine, Necker Hospital, Paris; ³Institut National de la Santé et de la Recherche Médicale Unit 559, Faculty of Medicine La Timone, Marseille; ⁴Laboratory HIF1H, UPRESS EA, University of Angers, Angers; and ⁵Vectorologie et Transfert de Gènes, Centre National de la Recherche Scientifique UMR 8121, Institut Gustave-Roussy, Villejuif, France

ABSTRACT

Radioiodine therapy of nonthyroid cancers after sodium iodide symporter (NIS) gene delivery has been proposed as a potential application of gene therapy. However, it seems to be precluded by the rapid efflux of taken up iodine from most transduced xenografted tumors. We present an *in vivo* kinetic study of NIS-related hepatic iodine uptake in an aggressive model of hepatocarcinoma induced by diethylnitrosamine in immunocompetent Wistar rats. We followed the whole-body iodine distribution by repeated imaging of live animals. We constructed a rat NIS (rNIS) adenoviral vector, Ad-CMV-rNIS, using the cytomegalovirus (CMV) as a promoter. Injected in the portal vein in 5 healthy and 25 hepatocarcinoma-bearing rats and liver tumors in 9 hepatocarcinoma-bearing rats, Ad-CMV-rNIS drove expression of a functional NIS protein by hepatocytes and allowed marked (from 20 to 30% of the injected dose) and sustained (>11 days) iodine uptake. This contrasts with the massive iodine efflux found *in vitro* in human hepatic tumor cell lines. *In vivo* specific inhibition of NIS by sodium perchlorate led to a rapid iodine efflux from the liver, indicating that the sustained uptake was not attributable to an active retention mechanism but to permanent recycling of the effluent radioiodine via the high hepatic blood flow. Radioiodine therapy after Ad-CMV-rNIS administration achieved a strong inhibition of tumor growth, the complete regression of small nodules, and prolonged survival of hepatocarcinoma-bearing rats. This demonstrates for the first time the efficacy of NIS-based radiotherapy in a relevant preclinical model of nonthyroid human carcinogenesis.

INTRODUCTION

Radioiodine (¹³¹I) therapy is a recognized, well-tolerated approach in the treatment of human thyroid cancer. Thyrocytes are physiologically capable of accumulating iodide attributable to the presence of the sodium iodide symporter (NIS) at their plasma membranes (1–4). Recently, NIS protein was found to be expressed in a large variety of cancers but was not located at the plasma membrane and had no significant iodide transport activity, except in breast cancer tissues (5, 6). To extend ¹³¹I therapy to nonthyroid cancers, gene therapy using NIS was proposed a few years ago (7–9). Various nonthyroid cancer cells (breast, cervix, lung, myeloma, and prostate) were transduced with NIS using plasmid-mediated transfection or virus-mediated gene delivery. High iodine uptake levels have indeed been achieved in these transduced cells both *in vitro* and in xenografted mice (10–12). Other studies report an almost total efflux of iodine from the cells, occurring less than 1 hour after the NIS-related uptake (13–16). Efflux was not significantly reduced by enzymatic or pharmacological means (14, 17–22). Interestingly, two studies have demonstrated a long

retention time for ¹²³I and significant tumor reduction after the application of a high dose of ¹³¹I in NIS-transduced mice (23, 24). However, all of these studies were performed in xenografted mice and not in the cancerous organs themselves, which limits their predictive potential for humans. The rapid efflux of iodine from nonthyroid cancer cells thus remains a major concern regarding the therapeutic applications of NIS gene transfer.

It should be noted that, *in vivo*, the tumor residence time of iodine results from a dynamic equilibrium between tumor cell uptake, efflux, and possible reuptake via the local blood supply and that this reuptake may compensate for a rapid efflux. On the basis of this observation, we have conjectured that the high hepatic blood flow in human liver and the hypervascular character of liver tumors might favor the reuptake of iodine and thereby increase significantly the lifetime of iodine in transduced hepatocytes. Therefore, *in vivo* quantitative organ-specific kinetic studies are required to validate NIS-based cancer gene therapy (25, 26). More specifically, it is necessary to perform quantitative follow-ups of the iodine distribution in transduced organs in pertinent preclinical models of cancer.

We report on a detailed study of NIS gene delivery via an adenovirus vector in the liver using a combination of *in vitro* experiments and *in vivo* investigations of rats presenting with chemically induced hepatocellular carcinoma induced by diethylnitrosamine. We found, for the first time, strong and sustained (several days) NIS-related radioiodine uptake in both normal and tumor-affected livers and an efficient inhibition of liver tumor growth after ¹³¹I therapy. Both *in vitro* and *in vivo*, and taking advantage of the specific inhibition of the NIS function by sodium perchlorate, we demonstrated that the prolonged uptake of iodine in the liver is not attributable to any active, liver-specific retention mechanism but is of a dynamic nature, meaning that it results from the balance between rapid efflux and intense reuptake promoted by high hepatic blood flow and NIS transduction. Taken overall, our results provide a new paradigm, which accounts for the *in vivo* efficacy of NIS gene delivery, and, thus, opens new prospects for the treatment of cancer using ¹³¹I therapy.

MATERIALS AND METHODS

Animals. Experiments were performed under the institutional and European Union guidelines for laboratory animal care. Hepatocarcinoma was induced in 6-week-old male Wistar rats weighing 150–180 g by the daily intake of diethylnitrosamine (Sigma-Aldrich, St. Louis, MO) in their drinking water (100 mg/L) for 8 weeks (27). The rats had received thyroxin (T4) supplementation (50 µg/L) in their drinking water to reduce unwanted thyroid iodine uptake. The litter was changed every other day to avoid fur contamination.

***In vivo* Gene Transfer.** Rats were anesthetized with intraperitoneal ketamine (120 mg/kg; Merck and Co. Inc., Whitehouse Station, NJ) and xylazine (20 mg/kg; Bayer AG, Leverkusen, Germany) and then laparotomized. Intraperitoneal adenovirus vector expressing NIS [adenovirus (Ad)-cytomegalovirus (CMV)-rat NIS (rNIS); ref. 10] was administered to 30 rats (5 healthy and 25 diethylnitrosamine-treated rats bearing tumor nodules with a diameter <5 mm). The rNIS vector was directly injected into 15, 5- to 10-mm diameter

Received 3/12/04; revised 8/17/04; accepted 8/24/04.

Grant support: Institut National de la Santé et de la Recherche Médicale, the Ligue Nationale contre le Cancer, and the Association pour la Recherche sur le Cancer.

The costs of publication of this article were defrayed in part by the payment of page charges. This article must therefore be hereby marked *advertisement* in accordance with 18 U.S.C. Section 1734 solely to indicate this fact.

Requests for reprints: Jamila Faivre, Inserm Unit 370, Faculty of Medicine Necker, 156 rue de Vaugirard, 75015 Paris, France. Phone: 33-1-40-61-56-44; Fax: 33-1-40-61-55-81; E-mail: faivre@necker.fr.

©2004 American Association for Cancer Research.

tumor nodules in 9 diethylnitrosamine-treated rats using a 30-gauge needle. In both cases, the administrated dose was of 5×10^9 infectious particles. Control animals received either 5×10^9 infectious particles of empty vector (Ad-DL324) or 500 μ L of saline buffer.

In vitro Iodine Uptake and Efflux Experiments. Huh7 and hepG2 liver cells were maintained in DMEM glutamax and a 50:50 mix of DMEM/F12K Ham's (Invitrogen Corp., Carlsbad, CA), respectively, supplemented with 10% bovine calf serum. The day before infection, 3×10^5 cells were seeded into 24-well dishes. Cells were incubated with Ad-CMV-rNIS at a multiplicity of infection of 10 for 24 hours. Iodine uptake and efflux studies were then performed as described previously (10, 28). The radioactive B-HBSS (Invitrogen) contained 1 μ Ci (37 kBq) of ^{123}I and 0.5 $\mu\text{mol/L}$ of NaI per well. For NIS inhibition studies, NaClO_4 was added at a concentration of 30 $\mu\text{mol/L}$.

In vivo Iodine Uptake Experiments. Planar scintigraphic imaging, Na^{123}I (Schering AG, Berlin, Germany) was injected intraperitoneally (6 to 12 MBq/rat). From 2 to 4 rats were imaged simultaneously using a high-resolution parallel collimator of either low or high energy for ^{123}I or ^{131}I imaging, respectively. Scintigraphic 256×256 images were obtained using a DSX gamma camera (GE, Waukesha, WI). The same procedure was applied serially for kinetic studies. We obtained higher resolution images by using a 4-mm hole pinhole collimator and increasing acquisition times and numerization.

Image Quantification. We used the region of interest method with appropriate background correction to calculate biological and effective uptake values. Organ half-lives were calculated using a mono-exponential fit.

Planning of Therapy. During a preliminary study, we had administered a fixed escalating schedule of ^{131}I activities (100, 300, and 650 MBq) in control and infected rats. Dosimetric data were obtained from early and late (≤ 7 days) uptakes. We set the dose absorbed in the liver at 40 Gy, because this dose had proved to be effective in the treatment of human hepatocarcinoma (29). The corresponding therapeutic activities were ~ 650 MBq for a mean liver weight of 20 g. This level of activity was well tolerated in control animals. No deaths had occurred after 3 months of follow-up, indicating that the bone marrow had not been ablated. Indeed, whole-body ^{131}I clearance followed a two-compartment model in our rats with a first effective half-life of ~ 30 hours (data not shown). We administered 650 MBq of ^{131}I to hepatocarcinoma-bearing rats intraperitoneally 2 weeks after the injection of Ad-CMV-rNIS.

In vitro Uptakes. Organ samples were weighed, radioactivity was measured in a well gamma counter, and the results expressed as a percentage of the injected dose per gram of tissue (%ID/g).

Histology, Immunofluorescence, Microautoradiography. Formalin-fixed tissue sections were embedded in paraffin, stained with H&E, and examined under a light microscope. For immunofluorescence, cryosections, 4 μm , were fixed in 4% paraformaldehyde for 15 minutes and incubated with a polyclonal antibody directed against amino acid 600 to 618 of rNIS diluted at 1:200 (10) for 1 hour, followed by fluorescein-conjugated donkey antirabbit antibody (Jackson ImmunoResearch Laboratories, Inc., West Grove, PA). Fluorescence was examined by UV fluorescence microscopy. ^{131}I -labeled liver sections were analyzed with a Micro-Imager (24×32 mm² field of view and 25 μm resolution; Biospace Mesures, Paris, France).

Statistics. Statistical comparisons were performed using variance analysis and a PLSD Fischer test at risk 5% (StatView 5.0 software SAS system).

RESULTS

In vitro Analysis of Iodine Uptake in Liver Cell Lines. Firstly, we evaluated the NIS function *in vitro* in hepatoma cells expressing rNIS, using radioiodine uptake assays. Fig. 1 demonstrates that CMV-rNIS-infected liver cells but not uninfected control cells were capable of taking up large quantities of iodine (≤ 100 times as much as control cells). The cellular concentration of ^{123}I reached its maximum 15 minutes after the start of incubation. This uptake was inhibited by sodium perchlorate, a potent inhibitor of active iodide transport, confirming that iodide uptake is essentially NIS dependent. However, an almost complete ($>90\%$) efflux of radioactivity was observed 5 minutes after withdrawal of the ^{123}I -containing medium. Thus, the uptake and release kinetics of iodine in NIS-expressing human cancer liver cell lines are essentially similar to those observed in transformed cell lines derived from other organs (14, 15).

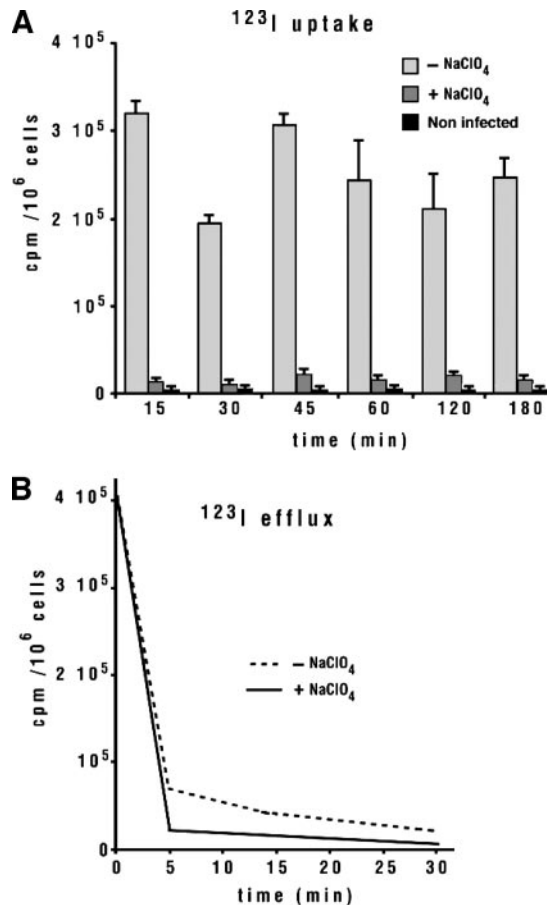
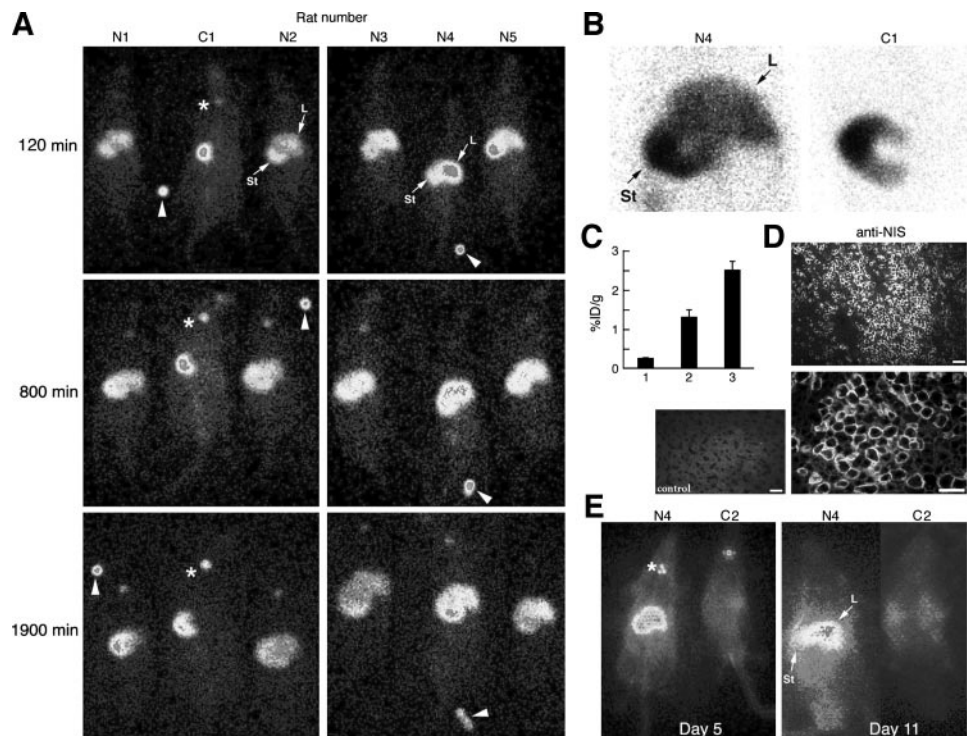


Fig. 1. *In vitro* uptake and efflux kinetics of ^{123}I in Ad-CMV-rNIS infected-Huh7 cells. A, uptake. Iodine activity measured at the indicated times after 60 minutes of incubation in a radioactive medium. B, efflux. Iodine activity measured at the indicated times after removal from the radioactive medium and washout. Each data point represents an average of four different experiments. -NaClO₄, without inhibition by sodium perchlorate. +NaClO₄, after inhibition by sodium perchlorate. Similar uptake and efflux kinetics have been observed in HepG2 cells.

In vivo Analysis of Iodine Uptake in NIS-Transduced Livers in Healthy Rats. We then assessed the global kinetics (biological liver uptake and residence times) in normal (Fig. 2) and hepatocarcinoma-bearing rats (Fig. 3) infected by the recombinant rNIS vector injected via the portal vein. Fig. 2 shows the time-dependent iodine liver uptake in infected and noninfected normal rats, visualized by serial ^{123}I scintigraphies. NIS is known to be physiologically expressed in thyroid, stomach, salivary glands, and lactating mammary glands (5, 30). We markedly inhibited iodide uptake in the thyroid gland by feeding the animals with water supplemented with thyroxin. The first image was taken at ~ 120 minutes post- ^{123}I injection, because dynamic studies showed that the injected activity was completely reabsorbed and urinary excretion negligible at that time (data not shown). A strong hepatic contrast was observed in the 5 infected rats (N1 to N5), whereas only a physiologic gastric contrast was visible in the noninfected rat C1 (Fig. 2A). The intensity of hepatic contrast varied from moderate (rat N1) to high (rat N4) but persisted until the end of the study (1,900 minutes, *i.e.*, 32 hours) in all of the infected rats. Thyroid uptake was low ($0.91 \pm 0.67\%$ ID at 120 minutes) in all of the animals because of thyroxin supplementation. No significant activity was observed in the bladder, which is the principal route of iodine elimination in mammals, indicating that plasma iodine concentrations were low because iodine was trapped in two accumulation sites (transduced liver and stomach) during the study. High-resolution pinhole images acquired at 1,900 minutes yielded clearly distinct

Fig. 2. *In vivo* kinetics of iodine uptake in healthy Wistar rats after the intraportal injection of Ad-CMV-rNIS. **A**, whole-body ^{123}I scintigraphy at the indicated times after ^{123}I injection using a gamma camera equipped with a parallel-hole collimator. Rats N1 to N5 were injected with 5×10^9 infectious particles *Rat C1*, control injected with 500 μL of PBS. ^{123}I was injected intraperitoneally 72 hours after viral or saline injection. *St*, stomach; *L*, liver; *, thyroid; *arrow*, internal standard of 0.5 MBq/50 μL . **B**, high-resolution pinhole collimator imaging of rats N4 and C1 at 1,900 minutes (31 hours) after ^{123}I injection. **C**, percentage of the ID/g counted 2 h after ^{123}I injection in the control (*column 1*) and in rats infected with 10^9 infectious particles (*column 2*) and 5×10^9 infectious particles (*column 3*) of Ad-CMV-rNIS. All differences in counts between the groups of rats were significant ($P < 10^{-4}$). **D**, anti-NIS immunofluorescence showing NIS expression in an infected rat liver. Note the targeting of NIS at the plasma membranes of transduced hepatocytes. Scale bars, 40 (20) μm in the top (bottom) image. Control, empty vector-infected rat. Scale bar, 40 μm . **E**, ^{131}I scintigraphy of rat N4 and an empty vector-infected rat (C2) at days 5 and 11 after ^{131}I injection. Rat N4 was representative of a batch of 20 animals. *St*, stomach; *L*, liver; *, thyroid.



images of the liver and stomach in NIS-infected rats (Fig. 2B; comparison of rat N4 with control C1). The pattern of liver uptake was always diffuse and homogeneous. The animals were sacrificed 1,900 minutes after ^{123}I injection, and the %ID/g was measured in liver samples (Fig. 2C). The liver ^{123}I concentration was high and viral-dose dependent, reaching $1.3 \pm 0.53\%$ ID/g for 10^9 infectious particles (column 2) and $2.5 \pm 0.64\%$ ID/g for 5×10^9 infectious particles (column 3) compared with the uptake reported in normal human thyroid glands of $\sim 1\%$ ID/g (31). In contrast, control rats (column 1) only exhibited low ($0.26 \pm 0.05\%$ ID/g, $P < 10^{-4}$) ^{123}I concentrations in the liver, which mainly reflected overall ^{123}I blood activity. We checked that rNIS protein was expressed at the surface of infected hepatocytes by immunofluorescence analysis in normal (Fig. 2D) and diethylnitrosamine-treated (Fig. 3C) rats. Thus, the iodine uptake observed was caused by a high level of NIS expression related to the strong transcriptional activity of the CMV promoter and adequate targeting of NIS to the plasma membrane of liver cells. On histologic examination at 3 weeks, the treated livers were normal without inflammatory infiltrates, apoptosis, or necrosis, indicative of the relatively strong radioresistance of normal hepatocytes to ^{131}I β particles (mean energy 606 keV; data not shown). Serial ^{131}I scintigraphy studies yielded similar, long-lasting (>11 days) iodine distributions in the livers of NIS-expressing rats, whereas distribution remained diffuse, with only a slight accumulation in the stomach, in control rats (Fig. 2E). The weak thyroid contrast (the residual uptake was 0.3% at day 5 and $<0.03\%$ at day 11) indicates stunning or destruction of the gland by ^{131}I attributable to the incomplete inhibition of thyroid uptake by thyroxine. Summarily, the delivery of Ad-CMV-rNIS to the normal liver through the portal vein drove the expression of a functional NIS protein *in vivo* and led to strong, sustained iodine uptake after infection.

***In vivo* Analysis of Iodine Uptake in NIS-Transduced Livers in Hepatocarcinoma-Bearing Rats.** We then examined rats bearing diethylnitrosamine-induced hepatocarcinoma (Fig. 3). As in normal rats, we injected 5×10^9 infectious particles of Ad-CMV-rNIS via the intraportal route. Fig. 3A shows a 24-hour serial whole-body ^{123}I

scintigraphy of two NIS-expressing hepatocarcinoma-bearing rats (D1 and D2), presenting with multinodular hepatocarcinoma. Fig. 3B shows a supplementary ^{131}I scintigraphy performed at 72 hours in 2 other hepatocarcinoma-bearing rats (D3 and D4) and a control rat (C3). The iodine uptake pattern exhibited specific hepatic and gastric contrast, similar to that observed in infected healthy rats. The hepatic contrast remained strong in late (≥ 72 hours) ^{131}I images, being even stronger than the gastric contrast (see rat D4), but was inhomogeneous, which was not surprising in view of the difficult, heterogeneous penetration of recombinant viruses in tumor cells (32). In control rats, only a weak gastric contrast appeared (see rat C3). Correlative *in vitro* ^{131}I counts demonstrated prolonged and strong uptake in tumor areas (Fig. 3D). The values observed ($8 \times 10^{-3}\%$ ID/g at day 8 and $10^{-2}\%$ ID/g at day 12, column 4) were 16 to 36 times higher than those measured in the plasma and normal liver ($<3 \times 10^{-4}\%$ ID/g, $P < 10^{-4}$, columns 1 and 5, respectively).

Time Evolution of Liver Iodine Uptake in Healthy and Hepatocarcinoma-Bearing Rats. We calculated the values of liver iodine uptake as a function of time using scintigraphy image quantification. The results obtained with ^{123}I are given in Fig. 4. Early (120 minutes) biological liver uptakes reached $36 \pm 6\%$ ID in infected healthy rats and $20 \pm 2\%$ ID in infected hepatocarcinoma-bearing rats *versus* $1.5 \pm 0.5\%$ ID in control rats ($P < 10^{-4}$). The cumulated uptakes were very high in infected healthy and hepatocarcinoma-bearing rats ($572 \pm 110\%$ hours and $294 \pm 50\%$ hours, respectively; $P < 0.016$) compared with control rats ($26 \pm 5\%$ hours; data not shown). It can be seen that the liver activity was lower in hepatocarcinoma-bearing than in healthy rats (but still much higher than in control rats), which was probably attributable to a relatively low transduction of tumor hepatocytes. However, even in hepatocarcinoma-bearing rats, liver uptake accounted for most of the whole-body ^{123}I activity at all times (Fig. 4B). Kinetic measurements were performed at late stages (3 to 11 days) by ^{131}I scintigraphy. We found a late biological half-life of iodine of 53 ± 9.2 hours in NIS-transduced liver. The cumulated uptakes were definitely higher in NIS-expressing rats ($1706 \pm 297\%$

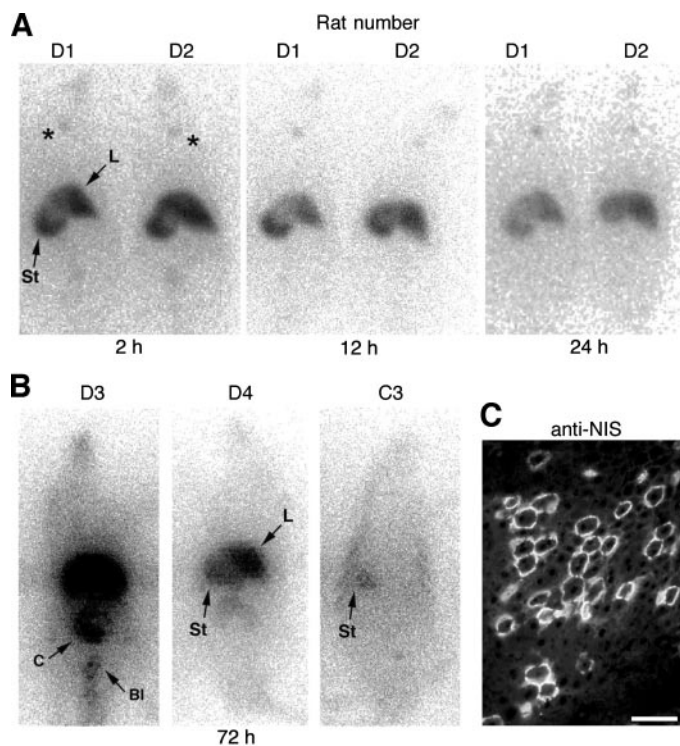


Fig. 3. Kinetics of iodine uptake after an intraportal injection of 5×10^9 infectious particles of Ad-CMV-rNIS in hepatocarcinoma-bearing rats (D1 to D4). Rat C3, hepatocarcinoma-bearing control rat infected with 5×10^9 infectious particles of an empty adenoviral vector. **A**, ^{123}I scintigraphy at the indicated times after the injection of ^{123}I . Same imaging procedure as in Fig. 2A. L, liver; St, stomach; *, thyroid. **B**, planar ^{131}I scintigraphy 72 hours after ^{131}I injection. L, liver; St, stomach; C, colon; Bl, bladder. Note the very strong radioiodine uptake in the liver of rNIS-infected rats. The hepatic area of the control rat showed no significant activity. Natural routes of ^{131}I elimination (colon and bladder) exhibited strong activity in rat D3. **C**, NIS expression in the liver of rat D1 visualized by immunofluorescence using an antibody anti-NIS. Scale bar, 20 μm . **D**, percentage of the ID/g 8 and 12 days after ^{131}I injection. Average values of a batch of 10 transduced hepatocarcinoma-bearing rats. 1, blood; 2, gastric mucosa; 3, gastric content; 4, injected tumor; 5, liver from three normal rats treated with ^{131}I . Gastric content versus injected tumor: $P < 10^{-4}$.

hours) than in controls ($324 \pm 114\%$ hours, $P < 0.0012$; data not shown).

Thus far, we had demonstrated a long-term retention of iodine in normal and cancerous liver after transfer of the *NIS* gene. This result clearly contrasts with the massive iodine efflux found *in vitro* by us in hepatic tumor cell lines (Fig. 1) and others in nonhepatic tumor cell lines. We additionally investigated this issue *in vivo* by studying liver iodine uptake kinetics after the injection of sodium perchlorate. Fig. 5 shows that ^{123}I hepatic contrast in Ad-CMV-rNIS-infected, hepatocarcinoma-bearing rats disappeared almost totally 6 minutes after drug injection. This establishes the absence of an active retention mechanism in transduced hepatocytes and strongly suggests that the long-term retention of iodine observed was mainly attributable to ^{123}I recirculation and reuptake.

Tumor Growth Inhibition in Hepatocarcinoma-Bearing Rats.

We investigated the inhibition of tumor growth after an intranodular injection of Ad-CMV-rNIS followed by intraperitoneal ^{131}I therapy

(650 MBq or 18 mCi). The volume of injected and noninjected nodules was measured 2 weeks after ^{131}I administration (Fig. 6A). The volume of injected nodules decreased or remained stationary (average decrease of 30%), whereas the volume of noninjected nodules grew significantly (average increase of 400%). Empty vector-injected nodules also exhibited a high growth rate (data not shown). Moreover, we observed that diffusion of the viral vector from the injected nodules prevented the development of new tumor nodules in the surrounding tissue, whereas this development was abundant in noninjected areas. This accounts for the relatively slow tumor growth observed in 2 rats (3 and 8), in which the noninjected nodules were all close to the injected nodule. Histologic analysis demonstrated apoptotic bodies and ballooning of hepatocytes in the Ad-CMV-rNIS-injected nodules (Fig. 6B). Micro-imager-based analysis showed heterogeneous low contrast inside the injected nodule, reflecting both reduced nodular vascularization and the loss of ^{131}I uptake activity in apoptotic cells (Fig. 6C). Doppler ultrasonography revealed dense vascularization in the perinodular area (data not shown), which may account for the enhanced contrast appearing in this area in Fig. 6C. The homogeneous labeling seen around the injected nodule illustrates diffusion of the NIS viral vector to nontumor liver.

Finally, we investigated the survival of hepatocarcinoma-bearing rats after treatment consisting of an injection of 5×10^9 infectious particles of Ad-CMV-rNIS via the portal vein followed by ^{131}I therapy (650 MBq or 18 mCi). In the absence of the latter, our diethylnitrosamine-treated rats exhibited the same median survival time as in previous studies (5 months after the onset of diethylnitrosamine administration; ref. 33). Eighteen diethylnitrosamine-treated rats were infected with Ad-CMV-rNIS, and ^{131}I was administered intraperito-

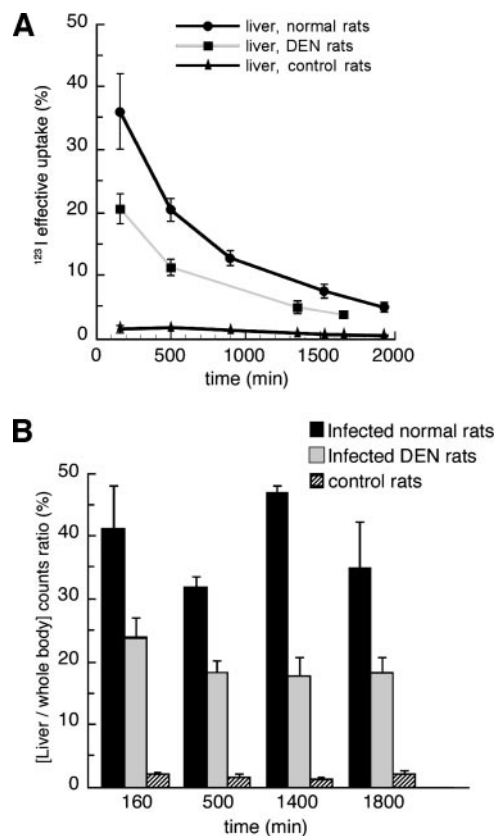


Fig. 4. Quantitative evaluation of iodine elimination kinetics in the livers of Ad-CMV-rNIS infected normal (healthy), hepatocarcinoma-bearing, and saline control rats. **A**, ^{123}I effective uptake. The curves are derived from scintigraphic images. Activity measurements were performed in the 5 normal rats (Fig. 2A) and 12 diethylnitrosamine-treated rats (Fig. 3A and data not shown). **B**, ratio of hepatic to whole-body activity after ^{123}I injection.

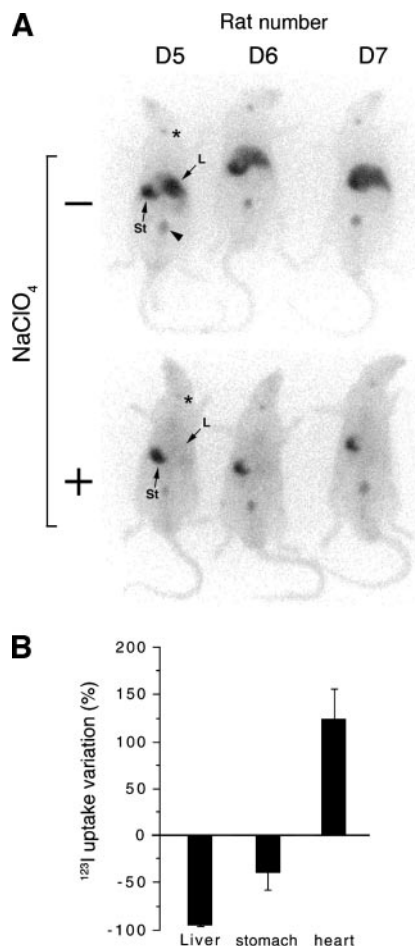


Fig. 5. *In vivo* inhibition of ^{125}I uptake after the injection of sodium perchlorate in NIS-infected, hepatocarcinoma-bearing rats (D5 to D7). A, top row (NaClO_4^-), whole-body scintigraphy images 120 minutes after ^{125}I injection. After this image acquisition, each rat was injected intraperitoneally with 100 mg of sodium perchlorate, and images were acquired at 1-minute intervals for 30 minutes. Bottom row (NaClO_4^+), whole-body scintigraphy images 15 minutes after the injection of sodium perchlorate. Note the absence of hepatic contrast and ^{125}I distribution throughout the body. L, liver; St, stomach; *, thyroid; arrow, ^{125}I injection site. B, ^{125}I relative variation in uptake before injection and 6 minutes after injection of sodium perchlorate in the indicated organs (mean values for 6 rats). The region of interest for the heart was delimited at time 1 min.

neally to 7 of them 3 months after the initiation (*i.e.*, 1 month after the end) of diethylnitrosamine administration at a time when the liver tumor nodules are microscopic. Survival was significantly increased in ^{131}I -treated rats (6 of 7 versus 1 of 11 for non- ^{131}I -treated rats at day 200; $P = 0.006$). The liver in the sole deceased ^{131}I -treated rat exhibited no macroscopic and histologic evidence of hepatocarcinoma (Fig. 6D).

These results establish the efficacy of ^{131}I treatment after NIS gene transfer in inhibiting the growth of large hepatic tumor nodules and preventing the formation of new tumor nodules in hepatocarcinoma-bearing rats. When the treatment is applied at a sufficiently early stage of the disease, it leads to a complete regression of tumor nodules and the improved survival of diethylnitrosamine-treated rats.

DISCUSSION

Our results provide clear evidence for the first time of the feasibility of obtaining, *in vivo*, high-level, long-lasting radioiodine uptake in NIS-expressing, nonthyroid cells. Using an adenoviral vector, we were able to strongly express a functional NIS at the plasma membrane of hepatocytes in normal and hepatocarcinoma-bearing rats. We

obtained a late biological half-life for iodine in the liver of these rats of 2.2 ± 0.4 days, which is adapted to the physical half-life of the widely used therapeutic radioisotope ^{131}I (8.05 days). On the other hand, we also showed *in vivo* that the iodine captured by hepatocytes rapidly left the liver cells when the symporter activity of NIS was inhibited by sodium perchlorate. Therefore, it is possible to conclude that the sustained radioiodine concentration in NIS-transduced hepatocytes was the result of a dynamic equilibrium among uptake, efflux, and reuptake. This high stationary liver iodine concentration was attributable, at least partly, to the high hepatic blood flow, which allows the rapid recycling of plasmatic radioiodine to the liver. Such a dynamic equilibrium between uptake and reuptake of the released drug, leading to high intracellular levels, has been reported for meta-iodobenzylguanidine, a structural analogue of noradrenaline, which targets neuroblastoma cells (34–36). Moreover, the large mass of NIS-expressing hepatocytes, attributable to the use of a strong ubiquitous promoter (CMV), favors cell-to-cell iodine reuptake. Another interesting aspect of our findings is that, in our experimental hepatocarcinoma model, long-term iodine retention in the liver occurred without the expression of thyroperoxydase, indicating that the cotransfer of thyroperoxydase with NIS would be unnecessary.

We also demonstrated that, in hepatocarcinoma-bearing rats, tumor growth was strongly inhibited and survival improved by ^{131}I therapy after NIS gene transfer. In fact, our results even suggest that a complete regression can be obtained in some cases. It is plausible that the immune response to the expressed NIS followed by ^{131}I therapy played a role in the survival of our treated immunocompetent animals, but this hypothesis will need to be specifically studied. The increased survival of our treated rats is highly significant given the extreme rapidity of spontaneous tumor progression in this hepatocarcinoma experimental model. We established the safety of this therapeutic procedure in both normal and hepatocarcinoma-bearing rats; all of the animals survived the maximum applied dose of 650 MBq of ^{131}I without developing bone marrow aplasia.

One of the current major challenges of gene therapy for cancer is the generally low transduction efficacy of tumor cells by the vectors used (37, 38). This has led to the concept that, regardless of the therapeutic approach proposed, a strong bystander effect will be necessary to allow the destruction of neighboring nontransduced tumor cells (39, 40). The intermediate path length of ^{131}I β emission (815 μm in water) may render ^{131}I an attractive candidate for such a bystander effect, because cross-fire irradiation can reach even non-transduced tumor hepatocytes. Our results support the validity of this concept by showing that hepatocarcinoma nodules with a diameter of <5 mm cease to grow and are partly destroyed by the presence of ^{131}I in some of the cells. Interestingly, micro-imager-based analysis of ^{131}I showed a marked strengthening in peritumor iodine uptake, a finding consistent with ^{131}I acting against tumor extension. Naturally, this beneficial effect was weaker in larger tumors in which the deposited dose was highly heterogeneous, although intranodular injection did evidence local antitumor action. Thus, our findings suggest that NIS-based, intraarterial gene therapy is indicated in cirrhotic livers with dysplastic and small tumor nodules, as well as in tumor recurrence after hepatocarcinoma resection; interestingly, in the latter case, intra-arterial lipiodol- ^{131}I has been shown to be efficient in reducing hepatocarcinoma recurrence and enhancing survival when administered after tumor resection (41). We did not observe any apparent ^{131}I -related liver damage in Wistar rats, although we were using a strong ubiquitous promoter (CMV), and the iodine liver uptake of normal transduced hepatocytes was higher than that of tumor ones (Fig. 4). Interestingly, the dose of 40 Gy used in our study is well tolerated by humans treated with ^{131}I -lipiodol (41). These results therefore suggest an increased sensitivity of liver tumor cells to

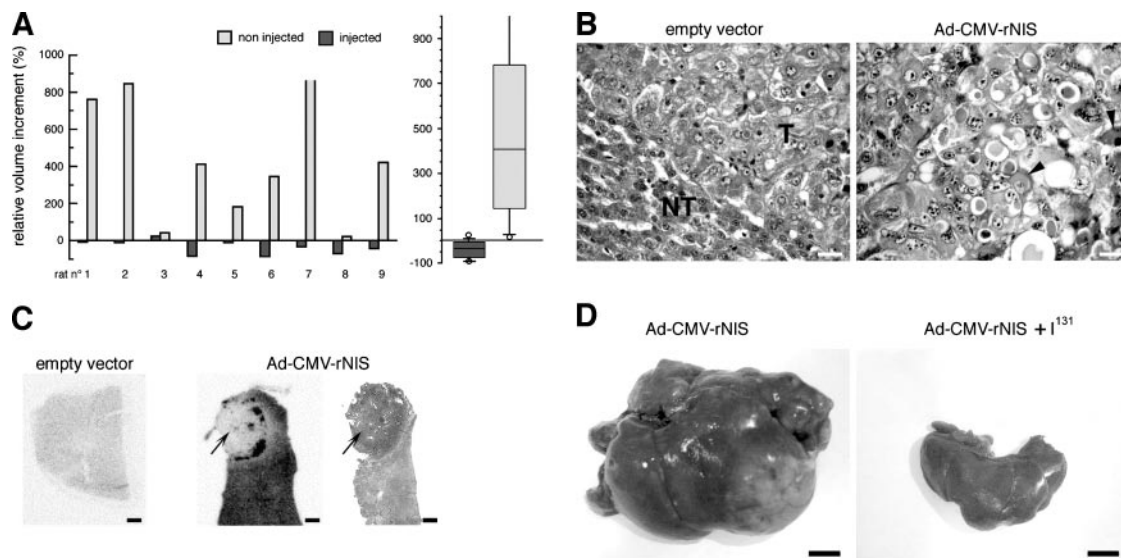


Fig. 6. Antitumor effect of ^{131}I therapy in hepatocarcinoma-bearing rats infected with 5×10^9 infectious particles of Ad-CMV-rNIS. *A, left*, tumor volume progression in injected and noninjected cancer nodules (9 rats). *Right*, changes to average tumor volumes. *B*, liver histology. *Arrows*, apoptotic bodies and ballooning of hepatocytes in an Ad-CMV-rNIS-injected nodule. The empty vector-injected nodule (*T*) exhibited basophilic staining and a high nucleocytoplasmic index. *NT*, noninjected tissue around the tumor. Scale bar, 20 μm . *C*, micro-imager-based analysis of ^{131}I distribution in liver sections of rats infected via the intranodular route. *Left*, empty vector-injected nodule. *Middle*, Ad-CMV-rNIS-injected nodule (*arrow*). Ad-CMV-rNIS yielded heterogeneous intranodular targeting with peri-nodular reinforcement. *Right*, liver histology of the same liver section. Scale bar, 1 mm. *D*, macroscopic views of a non- ^{131}I -treated (*left*) and ^{131}I -treated (*right*) rat liver 5 months after the initiation of diethylnitrosamine administration. The ^{131}I -treated liver was apparently cured of hepatocarcinoma nodules. Scale bar, 1 cm.

^{131}I compared with normal hepatocytes. Such conclusions might lead to use the strong CMV promoter when designing preclinical and clinical studies. However, we cannot exclude a late radiotoxicity occurring after our 2-month follow-up period, as observed in some patients. Thus, we still plan to test the targeting of NIS to tumor liver cells using tumor-specific promoters, such as α -foetoprotein (37). Moreover, this may improve the efficacy of our treatment in the case of large tumors by allowing selective increase of the irradiation dose in the tumor.

ACKNOWLEDGMENTS

We thank the Vector Core of the University Hospital of Nantes supported by the Association Française contre les Myopathies for producing the Ad-CMV-rNIS and DL324 vectors. We also thank J. M. Bidard for providing us with anti-rNIS antibody; F. Carnot for histological analyses of livers; J. M. Corr as for ultrasonography imaging; Y. Chr tien for statistical analyses; J. P. Djemat, A. Cavaill ez, C. Magnon, and M. Sichts for their technical help; and Biospace Mesures for kindly giving us access to a micro-imager.

REFERENCES

- Dai G, Levy O, Carrasco N. Cloning and characterization of the thyroid iodide transporter. *Nature* 1996;379:458–60.
- Smanik PA, Liu Q, Furminger TL, et al. Cloning of the human sodium iodide symporter. *Biochem Biophys Res Commun* 1996;226:339–45.
- Pinke LA, Dean DS, Bergert ER, Spitzweg C, Dutton CM, Morris JC. Cloning of the mouse sodium iodide symporter. *Thyroid* 2001;11:935–9.
- Selmi-Ruby S, Watrin C, Troutet-Masson S, et al. The porcine sodium/iodide symporter gene exhibits an uncommon expression pattern related to the use of alternative splice sites not present in the human or murine species. *Endocrinology* 2003;144:1074–85.
- Tazebay UH, Wapnir IL, Levy O, et al. The mammary gland iodide transporter is expressed during lactation and in breast cancer. *Nat Med* 2000;6:871–8.
- Wapnir IL, van de Rijn M, Nowels K, et al. Immunohistochemical profile of the sodium/iodide symporter in thyroid, breast, and other carcinomas using high density tissue microarrays and conventional sections. *J Clin Endocrinol Metab* 2003;88:1880–8.
- Mandell RB, Mandell LZ, Link CJ, Jr. Radioisotope concentrator gene therapy using the sodium/iodide symporter gene. *Cancer Res* 1999;59:661–8.
- De La Vieja A, Dohan O, Levy O, Carrasco N. Molecular analysis of the sodium/iodide symporter: impact on thyroid and extrathyroid pathophysiology. *Physiol Rev* 2000;80:1083–105.
- Spitzweg C, Harrington KJ, Pinke LA, Vile RG, Morris JC. Clinical review 132: the sodium iodide symporter and its potential role in cancer therapy. *J Clin Endocrinol Metab* 2001;86:3327–35.
- Boland A, Ricard M, Opolon P, et al. Adenovirus-mediated transfer of the thyroid sodium/iodide symporter gene into tumors for a targeted radiotherapy. *Cancer Res* 2000;60:3484–92.
- Kakinuma H, Bergert ER, Spitzweg C, Chevill e JC, Lieber MM, Morris JC. Probasin promoter (ARR(2)PB)-driven, prostate-specific expression of the human sodium iodide symporter (h-NIS) for targeted radioiodine therapy of prostate cancer. *Cancer Res* 2003;63:7840–4.
- Schipper ML, Weber A, Behe M, et al. Radioiodide treatment after sodium iodide symporter gene transfer is a highly effective therapy in neuroendocrine tumor cells. *Cancer Res* 2003;63:1333–8.
- Nakamoto Y, Saga T, Misaki T, et al. Establishment and characterization of a breast cancer cell line expressing Na⁺/I⁻ symporters for radioiodide concentrator gene therapy. *J Nucl Med* 2000;41:1898–904.
- Sieger S, Jiang S, Schonsiegel F, et al. Tumour-specific activation of the sodium/iodide symporter gene under control of the glucose transporter gene 1 promoter (GTI-1.3). *Eur J Nucl Med Mol Imaging* 2003;30:748–56.
- Haberhorn U, Kinscherf R, Kissel M, et al. Enhanced iodide transport after transfer of the human sodium iodide symporter gene is associated with lack of retention and low absorbed dose. *Gene Ther* 2003;10:774–80.
- Dadachova E, Carrasco N. The Na/I symporter (NIS): imaging and therapeutic applications. *Semin Nucl Med* 2004;34:23–31.
- Huang M, Batra RK, Kogai T, et al. Ectopic expression of the thyroperoxidase gene augments radioiodide uptake and retention mediated by the sodium iodide symporter in non-small cell lung cancer. *Cancer Gene Ther* 2001;8:612–8.
- Haberhorn U, Altmann A, Jiang S, Morr I, Mahmut M, Eisenhut M. Iodide uptake in human anaplastic thyroid carcinoma cells after transfer of the human thyroid peroxidase gene. *Eur J Nucl Med* 2001;28:633–8.
- Boland A, Magnon C, Filetti S, et al. Transposition of the thyroid iodide uptake and organification system in nonthyroid tumor cells by adenoviral vector-mediated gene transfers. *Thyroid* 2002;12:19–26.
- Spitzweg C, Scholz IV, Bergert ER, et al. Retinoic acid-induced stimulation of sodium iodide symporter expression and cytotoxicity of radioiodine in prostate cancer cells. *Endocrinology* 2003;144:3423–32.
- Kogai T, Schultz JJ, Johnson LS, Huang M, Brent GA. Retinoic acid induces sodium/iodide symporter gene expression and radioiodide uptake in the MCF-7 breast cancer cell line. *Proc Natl Acad Sci USA* 2000;97:8519–24.
- Schmutzler C. Regulation of the sodium/iodide symporter by retinoids—a review. *Exp Clin Endocrinol Diabetes* 2001;109:41–4.
- Dingli D, Peng KW, Harvey ME, et al. Image-guided radiotherapy for multiple myeloma using a recombinant measles virus expressing the thyroidal sodium iodide symporter. *Blood* 2003;103:1641–6.
- Spitzweg C, O'Connor MK, Bergert ER, Tindall DJ, Young CY, Morris JC. Treatment of prostate cancer by radioiodine therapy after tissue-specific expression of the sodium iodide symporter. *Cancer Res* 2000;60:6526–30.
- Groot-Wassink T, Aboagye EO, Glaser M, Lemoine NR, Vassaux G. Adenovirus biodistribution and noninvasive imaging of gene expression in vivo by positron

- emission tomography using human sodium/iodide symporter as reporter gene. *Hum Gene Ther* 2002;13:1723–35.
26. Groot-Wassink T, Aboagye EO, Wang Y, Lemoine NR, Reader AJ, Vassaux G. Quantitative imaging of Na/I symporter transgene expression using positron emission tomography in the living animal. *Mol Ther* 2004;9:436–42.
 27. Rajewsky MF, Dauber W, Frankenberg H. Liver carcinogenesis by diethylnitrosamine in the rat. *Science* 1966;152:83–5.
 28. Weiss SJ, Philp NJ, Grollman EF. Iodide transport in a continuous line of cultured cells from rat thyroid. *Endocrinology* 1984;114:1090–8.
 29. Zeng ZC, Tang ZY, Yang BH, et al. Comparison between radioimmunotherapy and external beam radiation therapy for patients with hepatocellular carcinoma. *Eur J Nucl Med Mol Imaging* 2002;29:1657–68.
 30. Welch PL, Mankoff DA. Taking up iodide in breast tissue. *Nature* 2000;406:688–9.
 31. Hooper PL, Turner JR, Conway MJ, Plymate SR. Thyroid uptake of ¹²³I in a normal population. *Arch Intern Med* 1980;140:757–8.
 32. Gerolami R, Cardoso J, Lewin M, et al. Evaluation of HSV-tk gene therapy in a rat model of chemically induced hepatocellular carcinoma by intratumoral and intrahepatic artery routes. *Cancer Res* 2000;60:993–1001.
 33. Peto R, Gray R, Brantom P, Grasso P. Effects on 4080 rats of chronic ingestion of N-nitrosodiethylamine or N-nitrosodimethylamine: a detailed dose-response study. *Cancer Res* 1991;51:6415–51.
 34. Smets LA, Janssen M, Metwally E, Loesberg C. Extracellular storage of the neuron blocking agent meta-iodobenzylguanidine (MIBG) in human neuroblastoma cells. *Biochem Pharmacol* 1990;39:1959–64.
 35. Clerc J, Mardon K, Galons H, et al. Assessing intratumor distribution and uptake with MBBG versus MIBG imaging and targeting xenografted PC12-pheochromocytoma cell line. *J Nucl Med* 1995;36:859–66.
 36. Brodeur GM. Neuroblastoma: biological insights into a clinical enigma. *Nat Rev Cancer* 2003;3:203–16.
 37. Sa Cunha A, Bonte E, Dubois S, et al. Inhibition of rat hepatocellular carcinoma tumor growth after multiple infusions of recombinant Ad.AFPtk followed by ganciclovir treatment. *J Hepatol* 2002;37:222–30.
 38. Kramer MG, Barajas M, Razquin N, et al. In vitro and in vivo comparative study of chimeric liver-specific promoters. *Mol Ther* 2003;7:375–85.
 39. McCormick F. Cancer gene therapy: fringe or cutting edge? *Nat Rev Cancer* 2001;1:130–41.
 40. Xue LY, Butler NJ, Makrigiorgos GM, Adelstein SJ, Kassis AI. Bystander effect produced by radiolabeled tumor cells in vivo. *Proc Natl Acad Sci USA* 2002;99:13765–70.
 41. Lau WY, Leung TW, Ho SK, et al. Adjuvant intra-arterial iodine-131-labelled lipiodol for resectable hepatocellular carcinoma: a prospective randomised trial. *Lancet* 1999;353:797–801.